

# Reverse-Engineered Highly Conformable, Leak and Pressure Reducing Cushion for Neonatal Resuscitation Mask

Carolyn M. McGann, Young-Joo Lee, Se-Um Kim, Danielle D. Weinberg, Xincheng Zha, Matthew Huber, Michael W. Hast, Kayley Dear, Vinay Nadkarni, Elizabeth E. Foglia,\* and Shu Yang\*

A significant proportion of newborn infants need facemask assisted resuscitation to start breathing successfully after birth. Positive pressure ventilation (PPV) is the most important intervention yet often impeded by facemask leak. A conformable, tacky silica gel that can be attached to the mask as a cushion is developed through reverse engineering. Finite element simulation reveals that the cushion forms a completely sealed interface while the mask alone without cushion has many potential leak sites. Since the cushion material is 20 times softer than the facial tissue, most deformation occurs in the cushion when applied, resulting in a fivefold lower contact pressure than using a conventional mask only. In a simulation trial with a realistic preterm manikin, the median mask leak for PPV inflations using the cushion is 15%, three times lower compared to that using the conventional mask alone, 44%. The median time to achieve leak-free is 16 s with the mask cushion, five times faster than that with standard mask, 81 s, allowing for more effective ventilation. This study offers promising insights on how the design of a 3D-contoured, soft silicone gel as the interface between a mask and a face can significantly improve neonatal resuscitation performance.

## 1. Introduction

Approximately 5–10% of all newborn infants require resuscitation to start breathing successfully immediately after birth.<sup>[1,2]</sup> The proportion of newborns receiving resuscitation increases with decreasing gestational age, with the majority of extremely preterm newborns requiring resuscitation after delivery.<sup>[2–4]</sup> Ventilation is the most important intervention during neonatal resuscitation but is challenging to perform effectively.<sup>[5]</sup> Two common impediments to providing effective facemask positive pressure ventilation (PPV) are mask leak and airway obstruction.<sup>[6–10]</sup> Delivered tidal volumes ( $V_t$ ) vary widely despite constant pressure settings, and mask leak may further contribute to variability in the delivered  $V_t$ .<sup>[8,11]</sup> This variability contributes to ineffective ventilation from both low  $V_t$  (leading to need for rescue tracheal intubation) and excessive  $V_t$  (leading to potential for lung injury). In

a simulated resuscitation on realistic manikins, providers apply excessive pressure to the facemask to achieve an adequate seal.<sup>[12]</sup> In clinical resuscitation, facemask application often precedes decreased heart rate, shallow breathing, or apnea.<sup>[13–15]</sup> This is thought to be mediated by the trigeminocardiac reflex from pressure activation of the highly innervated region surrounding the mouth and nose. The ideal facemask to deliver PPV would achieve and maintain a consistent seal with the face and require only minimal pressure applied.


Commercially available masks are anatomic or round in shape, have varying diameters from 35 to 60 mm, and have varied rim shapes; all are made with soft silicone.<sup>[16]</sup> Each of these mask characteristics can impact the seal formed with a neonate's face. Neither mask shape (anatomic or round), brand, or size consistently reduce mask leak.<sup>[17–21]</sup> Masks made with different materials have not been evaluated in published clinical trials. Commercially available masks for providing PPV in neonates have a flat contact region that does not conform well to a contoured human face. As a result, air leak could occur at the curved sites of the face, especially at concave or convex sites like the nasal bone or the boundary between the nose and cheek. Here, we develop a conformable mask interface with a soft contact region

C. M. McGann, D. D. Weinberg, M. Huber, E. E. Foglia,  
Division of Neonatology  
The Children's Hospital of Philadelphia  
3401 Civic Center Blvd., Philadelphia, PA 19104, USA  
E-mail: FOGLIA@chop.edu

Y.-J. Lee, S.-U. Kim, X. Zha, S. Yang  
Department of Materials Science and Engineering  
University of Pennsylvania  
3231 Walnut Street, Philadelphia, PA 19104, USA  
E-mail: shuyang@seas.upenn.edu

M. W. Hast, K. Dear,  
Biedermann Laboratory for Orthopaedic Research  
University of Pennsylvania  
3737 Market Street, Philadelphia, PA 19104, USA

V. Nadkarni  
Department of Anesthesiology  
Critical Care and Pediatrics  
The Children's Hospital of Philadelphia  
University of Pennsylvania Perelman School of Medicine  
3401 Civic Center Blvd., Philadelphia, PA 19104, USA

 The ORCID identification number(s) for the author(s) of this article can be found under <https://doi.org/10.1002/admt.202101364>.

DOI: 10.1002/admt.202101364

using a tacky material (Young's modulus  $\leq 100$  kPa, according to Dahlquist's criterion<sup>[22]</sup>) that would promote a mask seal with minimal pressure. An adequate fit of the mask is expected to maximize PPV efficiency as well as preventing skin stress and damage that may occur due to interface mismatch and contact pressure. Studies of personal protective equipment and noninvasive respiratory support masks have reported that skin injuries may occur at the sites where facial tissue is relatively thin such as the nasal bridge or cheekbones.<sup>[23–25]</sup>

Recent studies of shape programmable materials and wearable electronics fields have focused on how to conformally wrap uneven curved surfaces.<sup>[26–35]</sup> According to the Gauss theorem, the material is deformed through stretching, compression or tearing to develop a curved surface with nonzero Gaussian curvature.<sup>[26]</sup> Otherwise, wrinkles or voids are generated, causing delamination at the interface. To prevent delamination and maintain conformal wrapping, researchers have focused on enhancing the adhesion between the material and targeted surface. For example, thinner and more compliant materials are used to achieve better adhesion.<sup>[27,28]</sup> Stretchable and expandable *kirigami* structures incorporate a cut pattern to reconfigure the designated shape to be conformal to the substrate and improve the interface adhesion. These approaches increase the critical debonding energy release for delamination without changing the thickness and compliance of the adhesives.<sup>[29,30]</sup> We and others show geometrically designed fractal cuts can be utilized for wrapping an arbitrary 3D surface.<sup>[31–35]</sup> Nevertheless, *kirigami* approaches require stretching of the constituent materials to achieve conformal contact and adhesion, which is not suitable here since the standard mask cannot be stretched and is worn by compression against the neonate's face. Therefore, engineering a deformable interface based on compression to ensure conformability and thus a good seal between the mask and the neonatal face is highly desired.

As opposed to the flat and thin contact surface of standard masks, here we devise a few millimeters thick (to minimize buckling), soft and tacky cushion interfacing between a manikin face that is modeled after the neonatal face and the conventional mask. The preterm manikin used for these simulations has polyethylene bony structures with overlaying silicone skin. Although the tissue properties of these likely vary slightly from human tissues, silicones are widely used to study indentation, friction and blistering, and pressure injuries and have the advantage of producing contoured surface morphologies.<sup>[36–38]</sup> Since the cushion is designed with a targeted face contour at the cushion-face contact surface, it conforms to the face with minimal contact pressure and without localized stress generation, despite significant curvature of the facial surface profile. In addition, the innate tackiness of the cushion material improves seal, and the fact that the cushion is less stiff than facial tissue further reduces the contact pressure during application and use of the mask.

## 2. Results

### 2.1. Mask Fabrication

**Figure 1** shows the cushion manufacturing process through reverse engineering. First, a computer graphic model of the

face is generated through 3D scanning of a preterm manikin. From the scanned model, the contact surface of face-cushion interface is extracted (Figure 1A1, light blue). A model is designed and a mold is 3D printed to cast the silicone cushion with the extracted surface as one side, serving as the cushion-face interface (Figure 1A2). Since the contact part of the mask is flat, the cushion-mask interface is designed to be flat. The cushion is prepared from Ecoflex gel (Smooth-On), a silicone rubber that is known to be biocompatible and its Young's modulus can be varied to match or be smaller than that of facial tissues. Since the face is exposed to a vertical pressure with mask application, skin irritation may occur in areas with thin overlying skin if excessive contact pressure develops when applied.<sup>[24,25]</sup> When the resuscitation mask forms an adaptive interface under the applied compressive force, the softest material is deformed. To avoid tissue injury, a material for resuscitation facemasks should be softer than facial tissue, so that the deformation mainly occurs in the device when forming the adaptive interface.<sup>[39,40]</sup>

Young's modulus determines the stiffness of a material, which is associated with elastic deformation under elongation or compression. In this system, the Young's moduli of the thermoplastic elastomer constituting the standard mask, facial tissue, and Ecoflex gel are 3 MPa (obtained from mechanical testing results, Figure 1F), 790 kPa,<sup>[25]</sup> and 39 kPa, respectively.<sup>[41]</sup> Therefore, we can expect that most deformation will occur in the soft cushion when the mask is applied, and deformation of the facial tissue would be minimized. The casted Ecoflex gel cushion is then attached to the existing round resuscitation mask (Fisher and Paykel) (Figure 1B, cushion shaded in orange, see Experimental Section for Ecoflex gel preparation). Figure 1C–E shows a neonatal manikin with two standard masks (Carefusion anatomic-shaped and Fisher and Paykel round mask) and the standard mask with Ecoflex gel cushion. To investigate how the cushion improves the mask-face seal, we used finite element (FE) simulation to predict the degree of conformability and contact pressure level. The percentage of mask leak during PPV is experimentally measured in a manikin simulation trial.

### 2.2. Finite Element Simulation

**Figure 2** shows the FE simulation results predicting the appearance and contact pressure distribution on the face when applying three different types of masks to a preterm neonatal manikin. The simulations are performed for a standard round mask made with original thermoplastic polymer material (Fisher and Paykel model), a standard round mask made with Ecoflex gel, and a standard mask with an Ecoflex gel cushion attached. With the manikin face upward, the mask application process is simulated by applying the same amount of displacement to the mask model in contact with the face. With the same amount of indentation, we compare the appearance and the contact pressure levels on the manikin face (Figure 2C,F,I).

Figure 2A–C shows the appearance and contact pressure map on the face when the standard mask is applied. Since the face tissue is much softer than the constituting materials of the standard mask, to ensure a conformal contact, the facial

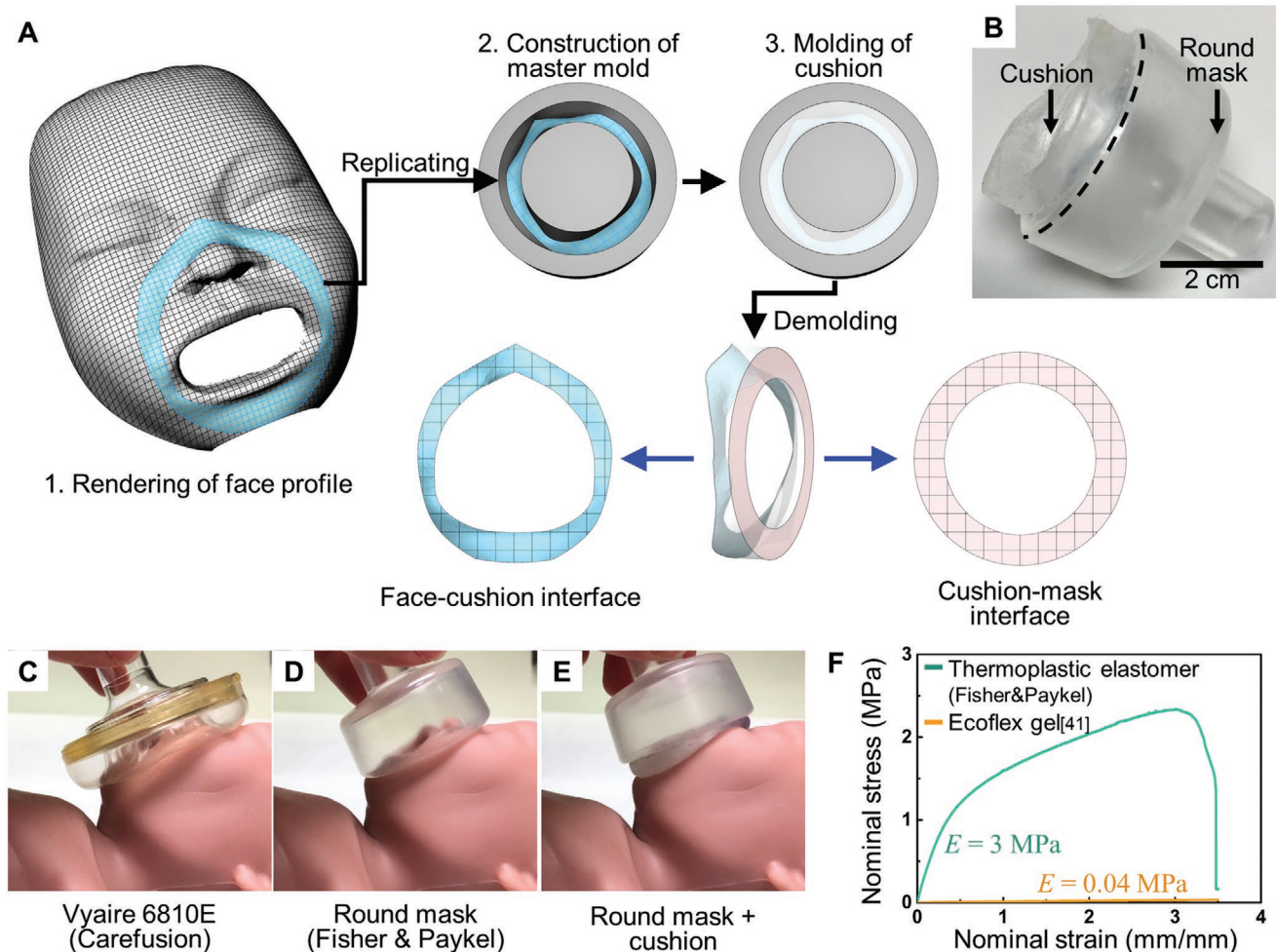


**Figure 1.** Design and fabrication of the mask cushion. A) Mask cushion fabrication process based on a preterm manikin model. B) A picture of the mask cushion attached to the standard round mask. C–E) Pictures of various types of commercial resuscitation masks on a preterm neonatal manikin. C) An anatomic mask (Carefusion). D) A standard round mask (Fisher and Paykel). E) A standard round mask with the Ecoflex gel mask cushion attached. F) Stress–strain curves of the soft cushion material (Ecoflex gel) and the thermoplastic elastomer used in the standard resuscitation mask (Fisher and Paykel).

tissue deforms leading to elevated localized contact pressure (Figure 2C). Contact-free areas are illustrated as a gray area in the pressure map. The incomplete contact pressure loop indicates a potential space for air leak, especially on the sides of the nose and provides space for air leakage. **Figure 3** displays the cross-sectional image of the simulated appearance of each mask model applied to the face. Figure 3B,C demonstrates that with the standard mask, the generated contact is incomplete especially on the sides of the nose. The slight overlap is due to the contact tolerance setting of the simulation, signifying that a relatively hard mask compresses soft tissue. This incomplete contact results from the significant curvature occurring at the boundary between the nose and the cheeks.

Figure 2D–F shows the contact morphology and contact pressure map of a standard mask made with Ecoflex gel. Under large enough compression, when only a single material is used, buckling occurs on the sidewall of the mask seen with both the standard mask and the Ecoflex mask (Figure 2B,E). A critical force that induces buckling is linearly proportional to Young's

modulus of the constituent material.<sup>[42]</sup> As stated previously, Young's modulus of Ecoflex gel and the thermoplastic elastomer of the standard mask are 39 and 4 MPa, respectively, thus a critical buckling force of the Ecoflex gel mask is  $\approx 100$  times lower than that of the standard mask. When a material softer than the tissue is used, we can expect to reduce the contact pressure level generated on the face (Figure 2F). However, since the mask itself is deformed, a proper contact surface is not formed. As a result, we would expect a large mask leak. This can also be seen in the cross-sectional image in Figure 3E,F which demonstrates incomplete contact around the nose and a very narrow width of contact below the mouth due to deformation of the mask.

It is reasonable to expect lower contact pressure levels when using soft materials to make a resuscitation mask. However, the comparison of Figure 2C,F suggests that a problem may occur in terms of air leak especially around the nose. From these results, we can see that it is essential to use a material softer than the tissue to decrease contact pressure on the face.

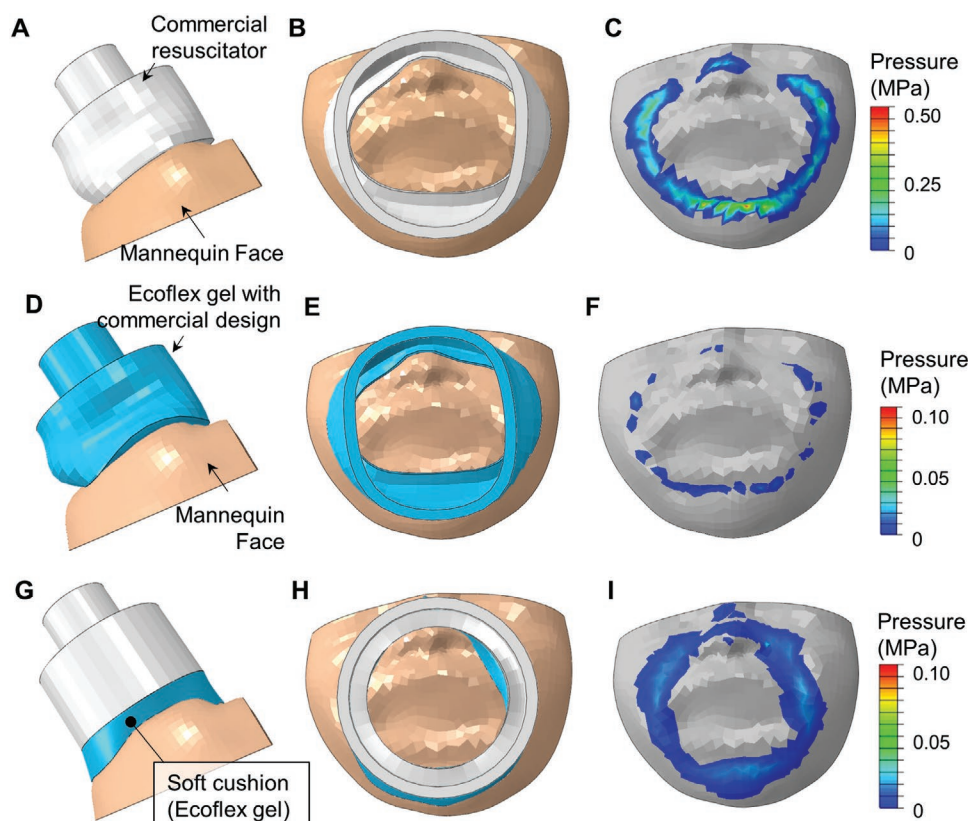


**Figure 2.** Finite element simulation of the contact pressure applied to a preterm neonatal manikin face using three different types of masks. A) Side and B) top views of a standard round mask applied to the face. C) The contact pressure contour on the manikin face. Compared to other masks, the highest contact pressure is generated in this simulation with standard mask. D) Side and E) top views of a round mask made of Ecoflex gel. F) Contact pressure contour on the manikin face. G) Side and H) top views of a standard round mask with an attached Ecoflex mask cushion. I) Contact pressure contour on the manikin face. A closed loop indicates that a full seal is achieved between the cushion and the face. In (C), (F), and (I), the gray areas indicate that no contact occurs in this area.

However, replacing only the material with the same mask architecture does not solve the Gaussian theorem problem of how a flat contact surface conforms to a curved face.

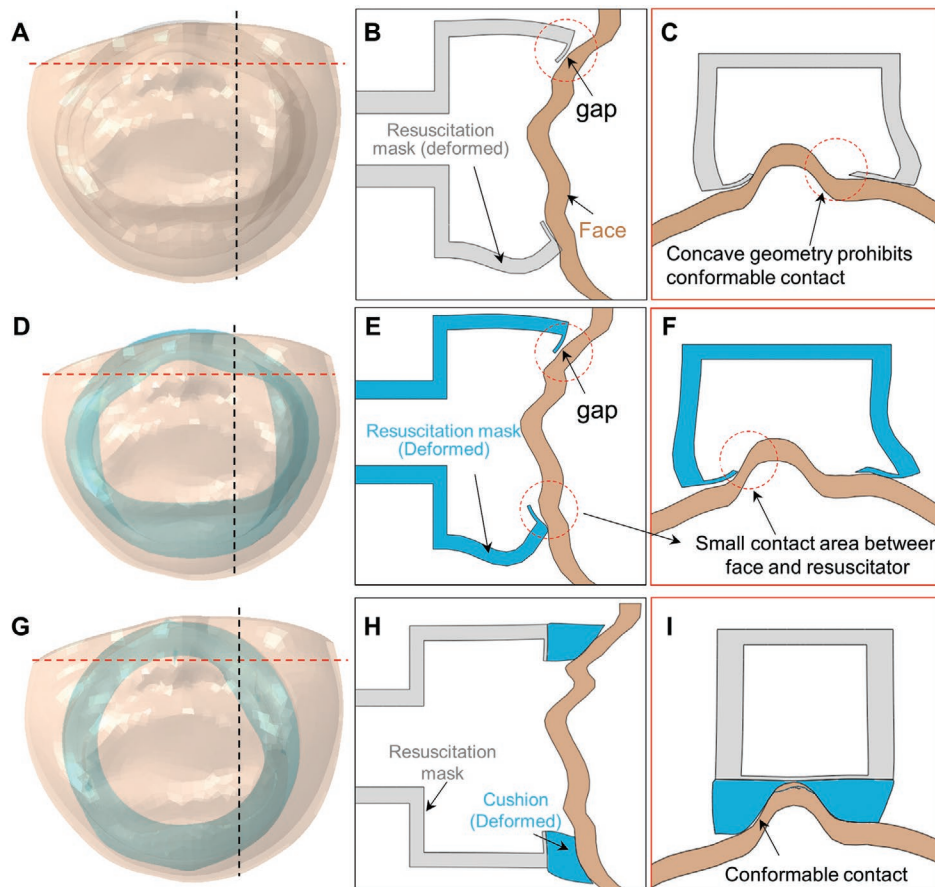
Unlike masks made of a single material, when attaching a thick Ecoflex gel cushion to a standard mask, buckling of the mask sidewall does not occur; instead, all deformation is concentrated in the Ecoflex gel cushion during application. Therefore, the localized contact pressure on the face is diminished. For example, the contact pressure level with the Ecoflex gel cushion is around 0.05 MPa (Figure 2I), which is five times lower than that with a standard mask demonstrated around 0.25 MPa pressure level in the contact area (Figure 2C). Importantly, with the Ecoflex cushion the contact area forms a closed loop, indicating that the gel cushion is able to form an adaptive contact surface after application and we would expect mask leak to be minimized. This result is in sharp contrast to the simulation with a standard mask (Figure 2C), where stress localization occurs with increased contact pressure at the cheeks and chin and no contact on either side of the nose preventing a complete seal. Also, it is contrary to the simulation with an Ecoflex gel mask (Figure 2F), which shows large contact losses due to deformation during compression.

Figure 3H,I shows that the Ecoflex gel cushion closely adheres to the face when compressed, creating a good adaptive

interface. From FE simulation results, we can expect that a mask made from material that is softer than tissue will allow for a more adaptive contact surface and decreased mask leak. However, when the entire resuscitation mask is made from the soft Ecoflex material, buckling will occur during use. When the standard mask is combined with a soft Ecoflex cushion, we can combine the beneficial characteristics of each material to generate complete contact without significant deformation of the mask nor buckling.

### 2.3. Manikin Simulation Trial

We conducted a proof-of-principle simulation trial of neonatal providers to determine if PPV performed with a standard mask coupled with a mask cushion, compared to PPV performed with a standard mask reduces the primary outcome of percent mask leak. There are 33 enrolled participants with a mean age of 32 years; 18 are randomized to start with the mask cushion. Most participants are female, as the first-year neonatology fellows and have completed residency in the past year (Table 1). All participants have complete data recorded on the respiratory function monitor (RFM). We note that the washout period was less than 90 s for five participants (ranging from 40–75 s).



**Figure 3.** Finite element simulations showing the contact shapes of standard mask, Ecoflex round mask, and round mask with attached cushion on preterm neonatal manikin. The box color (black or red) corresponds to the cross section of the dashed lines in (A), (D), and (G). A) A semi-transparent top-view with a standard round mask. B,C) Cross-section of the standard mask model at the intersection of dashed lines in panel (A). Due to the concave shape of the face, the standard mask forms imperfect contact and gaps remain which can be a source of mask leak. D) Semi-transparent top-view with a round mask made with Ecoflex gel. E,F) Cross-section of the Ecoflex mask model at the intersection of dashed lines in panel (D). G) Semi-transparent top-view with a standard mask with attached cushion. H,I) Cross-section of the mask cushion model at the intersection of dashed lines in panel (G). When attached on the face, the soft cushion is compressed at a low enough contact pressure to form a conformable contact without gaps and voids.

These participants' results are still included in the analysis. The mean number of PPV inflations delivered during each simulation does not differ between arms, 69 (mask cushion) and 70 (standard mask).

The median mask leak for PPV inflations is significantly lower for PPV performed with the mask cushion, 15% (interquartile range, IQR, 1–46%), compared with standard mask (44%, IQR 33–80%,  $p < 0.05$ , **Figure 4A**). In addition, PPV inflations performed with the mask cushion have a statistically lower proportion of breaths with significant leak, and higher median expiratory tidal volume ( $V_{te}$ ) (Figure 4C). The median time to achieve leak-free mask seal is 16 s with mask cushion compared to 81 s with standard mask (log rank test,  $p = 0.05$ , **Figure 4B**).

### 3. Discussion/Conclusion

This study shows that a conformable 3D-printed mask interface reduces mask leak in a simulation setting with a preterm manikin and decreases the contact pressure required to form

a complete seal in FE simulations. Masks have previously been designed as flat surfaces that are meant to conform to the contours of a human face. Using 3D renderings of human faces and preterm manikins, we 3D print molds that allow for casting a 3D-contoured cushion for better fit to the target faces. This technique allows us to use a softer and more conformable material which can be compressed to form a more adequate seal. At birth, an individualized 3D printed mask would not be feasible as resuscitation with PPV needs to be given within the first minute of life. The engineered mask interface is designed to be compressible enough to form a seal accounting for individual differences in facial dimensions. As preterm neonates are the most likely population to require resuscitation after delivery, equipment development should focus on this population. For this reason, we choose to test the mask cushion on a preterm manikin. Until now, no mask has shown consistent superiority in reducing mask leak.

Mask leak is a major impediment to adequate ventilation and is nearly ubiquitous during neonatal resuscitation. With the mask cushion, neonatal providers can achieve a seal with a lower median leak during PPV, and the time to achieve this

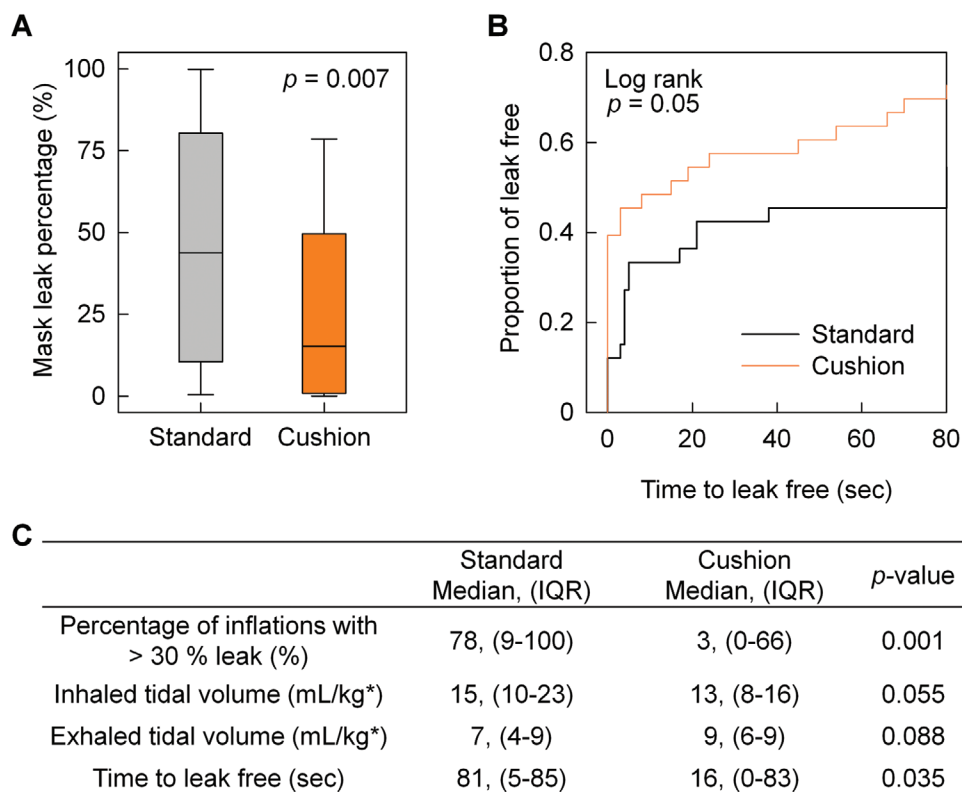
**Table 1.** Participant demographics and PPV experience.

Variable	All participants (n = 33)	
Age (years), mean (Standard Deviation)	32.1 (2.5)	
Sex, n (%)	Female	27 (79)
	Male	6 (18)
Postresidency years of experience, n (%)	0	19 (57)
	1	6 (18)
	2	5 (15)
	>3	3 (9)
	Previous equipment and practice used during delivery room PPV	
Typically used masks, <sup>a)</sup> n (%)	Anatomic	11 (33)
	Round, Laerdal	5 (15)
	Round, Fischer and Paykel	14 (42)
	Unsure	8 (24)
Typically used ventilation equipment, <sup>a)</sup> n (%)	T-piece resuscitator	31 (94)
	Self-inflating bag	2 (6)
	Flow-inflating bag	7 (21)
Typically used mask hold, n (%)	One hand hold	17 (51)
	Two hand hold	16 (48)

<sup>a)</sup>Participants could choose all options that applied.

seal is significantly shorter. As mask leak can occur many discrete times during neonatal resuscitation, achieving a leak-free seal more quickly could allow for more time spent delivering adequate ventilation during resuscitation.

We note the study is limited to the simulation setting, and the compressibility of the face of a manikin is likely not the same as that of a human neonate. Additionally, human neonates often have a layer of vernix or other secretions on their faces after delivery. This would change the surface of contact with the mask cushion but would have been hard to simulate uniformly in a trial with manikins or human neonates. It is possible that providers may perform PPV differently in the clinical setting with other distractions such as monitors, other team members, and ongoing clinical care. Similarly, the contact surface of a human neonate's face may change with grimacing of the facial muscles or crying. We believe that the compressibility of the mask cushion would allow it to maintain a contact interface; however, this would need to be evaluated in a clinical trial. Testing the mask cushion performance in a clinical setting could further validate and optimize the cushion design in the future. Importantly, this study offers new insights that incorporating a 3D contoured, soft, and deformable silicone gel as the interface between a conventional mask and face could significantly improve neonatal resuscitation performance of conventional masks.



\*Using estimated weight for manikin

**Figure 4.** Results of manikin simulation trial ( $n = 33$ ). A) The results of the primary outcome, mask leak percentage (Wilcoxon signed rank test,  $p = 0.007$ ). B) The time to achieve leak-free seal in the standard mask and mask cushion (log rank test,  $p = 0.05$ ). C) Results of secondary outcomes: percentage of inflations with >30% leak, inspiratory tidal volume, expiratory tidal volume, time to leak free (Wilcoxon signed rank test,  $p$ -values as listed in table).

## 4. Experimental Section

**Mask Design and Fabrication:** In the general fabrication process of the mask cushion, a 3D rendering of an infant face is derived by scanning (Artec Space Spider; Artec 3D) a preterm manikin face. This 3D rendering is then adjusted to produce a master mold. Adjustments are influenced by 3D smoothed rendering of infant faces from a radiologic image repository and through an iterative process of testing the mask cushion prototype on multiple manikins with varying face shapes. Master molds that replicate the face profile surrounding the mouth and the nose on the bottom surface are constructed using a 3D printer (Ultimaker 3, Ultimaker, Netherlands) with a filament of acrylonitrile butadiene styrene copolymer. Silicone prepolymers of Ecoflex Gel (1:1 wt% ratio of Part A and Part B) for the fabrication of the mask cushion body are casted on the prepared master molds, cured at room temperature for 1 h, and postannealed at 60 °C for 2 h. Mask cushions of cured silicone are manually demolded from master molds. Mask cushions are bonded on standard round masks. The preterm mask cushion has a 38 mm outer and 25 mm inner radius with a width of 13 mm. The term mask cushion has a 70 mm outer and 50 mm inner radius with a width of 20 mm. The height from cheek to mask of both mask cushions vary from 3.5 mm to 7.5 mm, as it is modeled to follow the contours of the face.

**Finite Element Simulation of Mask Cushion:** FE simulations are conducted through ABAQUS/Explicit solver to estimate the contact morphology and the distribution of contact pressure when using each mask configuration. Three different cases are simulated; first is a standard round resuscitation mask, second is a theoretical mask made of Ecoflex gel with standard round design, third is a standard mask with attached Ecoflex gel cushion. Linear elastic properties are applied to the thermoplastic elastomer constituting the standard mask material and Ecoflex gel. Young's modulus and Poisson's ratio of the thermoplastic elastomer of standard mask are 3 MPa and 0.49, and those of Ecoflex gel are 39 KPa and 0.495,<sup>[41]</sup> respectively. The stress–strain curves of standard materials were obtained by tensile test (Figure 1F). A preterm neonatal face model was prepared by computer-aided design with 3D scanning of a manikin to have 5 mm tissue thickness. Young's modulus and Poisson's ratio of tissue material is assumed 790 kPa and 0.42, respectively according to the literature.<sup>[43]</sup> C3D8 mesh is applied to the mask and face model and C3D10M mesh is applied to the soft cushion. Compression is applied to the preterm neonatal face model through displacement control of the mask (Figure S1, Supporting Information).

**Manikin Simulation Trial: Enrollment and Consent:** This is a randomized crossover simulation trial at The Children's Hospital of Philadelphia of neonatal fellows recruited from many fellowship programs. The Children's Hospital of Philadelphia Institutional Review Board approved this study. Participants are consented as a group and are eligible to participate after they attended a session introducing the standard resuscitation equipment. Only neonatal fellows were included in this study as prior evidence showed conflicting effects of provider experience level on mask leak.<sup>[17,44]</sup>

**Experimental Setup:** The experimental setup is the same for both arms of the trial. A preterm neonatal manikin (Premature Anne, Laerdal, Stavanger, Norway) is confirmed to be leak-free using the RFM (described below). A T-piece resuscitator (Neopuff, Fisher and Paykel Healthcare, Auckland, New Zealand) is set with a peak inspiratory pressure (PIP) of 20 cm H<sub>2</sub>O, positive end-expiratory pressure (PEEP) of 5 cm H<sub>2</sub>O using a flow of 10 L min<sup>-1</sup>. The T-piece is attached to a round mask, size small (Infant Resuscitation mask, Fisher and Paykel Healthcare, Auckland, New Zealand) for the control arm and the same sized facemask plus novel mask cushion for the intervention arm. Subjects are randomly assigned to perform PPV with either the facemask plus mask cushion or standard facemask first. The randomization scheme is generated with STATA 15.1 (Statacorp, College Station, TX).

Respiratory measurements of all PPV inflations are recorded with an RFM (New Life Box, Advanced Life Diagnostics, Weener, Germany) with an in-line flow sensor (Avea VarFlex Flow Transducer: CareFusion, Yorba Linda, California, USA). The RFM integrates signals from the flow sensor and collects data including respiratory rate, flow, PIP, PEEP,

inspiratory ( $V_{ti}$ ) and expiratory tidal volumes ( $V_{te}$ ), and mask leak. The RFM is not visible to participants as it is not used routinely in neonatal clinical practice and has been shown to affect mask leak percentage when visible.<sup>[45]</sup>

**Experimental Conditions:** Each participant receives standardized and scripted instructions directing them to provide PPV with the technique they normally would when performing single provider PPV for an apneic preterm neonate. They can ask questions but cannot touch the equipment before the PPV assessment is started. Once all questions are answered, participants perform PPV for 90 s with the first randomly assigned interface. Following a 90 s washout rest period, each participant performs PPV for 90 s with the second interface.

**Statistical Analysis:** Inflations are analyzed using breath-by-breath analysis (Pulmochart Software 4.24, Advanced Life Diagnostics, Germany). The data from all participants were used for each analysis and were not normalized or transformed prior to statistical analysis. The primary outcome is mask leak, calculated using the following equation:  $(V_{ti} - V_{te})/V_{ti} \times 100$ . Secondary outcomes are  $V_{te}$  and proportion of inflations with significant mask leak (defined as mask leak > 30%), time to leak free (defined as three consecutive breaths with < 30% mask leak). The sample size is calculated for the primary outcome, percent mask leak. Assuming that the standard deviation of the paired differences is 20% for the primary outcome, 30 participants are needed to have 80% statistical power to detect a difference of 10.6% in percent mask leak with a significance level of 0.05. Using R V3.6.3, summary statistics are generated for participant demographics and inflation data. Outcomes are compared between interfaces using a Wilcoxon signed rank test to compare medians and a log rank test to compare time to leak-free. A  $p$ -value < 0.05 is considered statistically significant.

## Supporting Information

Supporting Information is available from the Wiley Online Library or from the author.

## Acknowledgements

The seed fund from Penn Health-Tech (to E.E.F. and S.Y.) is acknowledged to support the work reported here. Y.-J.L. was supported on Accelerating from Lab to Market grant from University Research Foundation at University of Pennsylvania (to S.Y.). The authors gratefully acknowledge the use of Instron supported by the Department of Materials Science and Engineering Departmental Laboratory at the University of Pennsylvania.

## Conflict of Interest

E.E.F., D.D.W., S.-U.K., and S.Y. have an interest in the “Neonatal Mask Cushion” intellectual property described in this study, which is jointly held by Children's Hospital of Philadelphia and University of Pennsylvania.

## Author Contributions

C.M.M., Y.-J.L., S.-U.K., and D.D.W. contributed equally to this work. S.Y. and E.E.F. contributed equally to this work. D.D.W., E.E.F., and S.Y. conceived the idea of the cushion interface. S.-U.K. designed and fabricated the mask cushions and X.Z. participated in the iterative mask cushion fabrication. Y.-J.L. performed FE simulations and mechanical testing. C.M.M. performed manikin simulation trial. V.N. contributed to the simulation trial design and data interpretation. M.W.H., S.-U.K., and Y.-J.L. analyzed the data. C.M.M., S.-U.K., Y.-J.L., and D.D.W. wrote the paper. K.D. and M.W.H. developed pressure equipment. All authors discussed the data and commented on the paper. C.M.M., Y.-J.L., S.-U.K., D.D.W., E.E.F., and S.Y. critically revised the paper.

## Data Availability Statement

The data that support the findings of this study are available from the corresponding author upon reasonable request.

## Keywords

contact pressure, facemask, neonate, resuscitation, seal cushion

Received: October 16, 2021

Revised: December 1, 2021

Published online:

- [1] J. Wyllie, J. M. Perlman, J. Kattwinkel, M. H. Wyckoff, K. Aziz, R. Guinsburg, H. S. Kim, H. G. Liley, L. Mildenhall, W. M. Simon, E. Szlyd, M. Tamura, S. Velaphi, D. W. Boyle, S. Byrne, C. Colby, P. Davis, H. L. Ersdal, M. B. Escobedo, Q. Feng, M. F. de Almeida, L. P. Halamek, T. Isayama, V. S. Kapadia, H. C. Lee, J. McGowan, D. D. McMillan, S. Niermeyer, C. P. F. O'Donnell, Y. Rabi, S. A. Ringer, N. Singhal, B. J. Stenson, M. L. Strand, T. Sugiura, D. Trevisanuto, E. Udaeta, G. M. Weiner, C. L. Yeo, *Resuscitation* **2015**, *95*, e169.
- [2] M. H. Wyckoff, K. Aziz, M. B. Escobedo, V. S. Kapadia, J. Kattwinkel, J. M. Perlman, W. M. Simon, G. M. Weiner, J. G. Zaichkin, *Circulation* **2015**, *132*, S543.
- [3] R. Guinsburg, M. F. de Almeida, J. S. de Castro, W. A. Goncalves-Ferri, P. F. Marques, J. P. Siqueira Caldas, V. L. Jornada Krebs, L. M. de Souza Rugolo, J. H. C. Leme de Almeida, J. H. Luz, R. S. Procianny, J. L. M. Bandeira Duarte, M. Gomes Penido, D. M. de Lima Mota Ferreira, N. Alves Filho, E. M. de Albuquerque Diniz, J. P. Santos, A. L. Acquesta, C. Nunes dos Santos, M. R. Conde Gonzalez, R. P. V. Cavalvanti da Silva, J. Meneses, J. M. de Andrade Lopes, F. E. Martinez, *Arch. Dis. Child. Fetal Neonat. Ed.* **2018**, *103*, F49.
- [4] N. Kumbhat, B. Eggleston, A. S. Davis, K. P. Van Meurs, S. B. Demauro, E. E. Foglia, S. Lakshminrusimha, M. C. Walsh, K. L. Watterberg, M. H. Wyckoff, A. Das, S. C. Handley, *Arch. Dis. Child. Fetal Neonat. Ed.* **2021**, *106*, 62.
- [5] F. E. Wood, C. J. Morley, *Semin. Fetal Neonat. Med.* **2013**, *18*, 344.
- [6] J. J. van Vonderer, H. Ad. van Zanten, K. Schilleman, S. B. Hooper, M. J. Kitchen, R. S. G. M. Witlox, A. B. Te Pas, *Front. Pediatr.* **2016**, *4*, 38.
- [7] E. E. Foglia, A. B. te Pas, *Semin. Fetal Neonat. Med.* **2018**, *23*, 340.
- [8] G. M. Schmölzer, J. A. Dawson, C. O. F. Kamlin, C. P. F. O'Donnell, C. J. Morley, P. G. Davis, *Arch. Dis. Child. Fetal Neonat. Ed.* **2011**, *96*, F254.
- [9] K. Schilleman, R. S. Witlox, E. Lopriore, C. J. Morley, F. J. Walther, A. B. te Pas, *Arch. Dis. Child. Fetal Neonat. Ed.* **2010**, *95*, F398.
- [10] N. N. Finer, W. Rich, C. Wang, T. Leone, *Pediatrics* **2009**, *123*, 865.
- [11] G. M. Schmölzer, O. C. O. F. Kamlin, J. A. Dawson, A. B. Te Pas, C. J. Morley, P. G. Davis, *Arch. Dis. Child. Fetal Neonat. Ed.* **2010**, *95*, F295.
- [12] J. J. van Vonderer, T. A. Kleijn, K. Schilleman, F. J. Walther, S. B. Hooper, A. B. te Pas, *Arch. Dis. Child. Fetal Neonat. Ed.* **2012**, *97*, F254.
- [13] K. L. A. M. Kuypers, T. Lamberska, T. Martherus, J. Dekker, S. Böhlinger, S. B. Hooper, R. Plavka, A. B. te Pas, *Resuscitation* **2019**, *144*, 178.
- [14] V. D. Gaertner, C. M. Rüggeger, E. O'Curraïn, C. O. F. Kamlin, S. B. Hooper, P. G. Davis, L. Springer, *Arch. Dis. Child. Fetal Neonat. Ed.* **2021**, *106*, 381.
- [15] K. L. A. M. Kuypers, T. Lamberska, T. Martherus, J. Dekker, S. Böhlinger, S. B. Hooper, R. Plavka, A. B. te Pas, *Resuscitation* **2020**, *157*, 60.
- [16] S. Machumpurath, E. O'Curraïn, J. A. Dawson, P. G. Davis, *Resuscitation* **2020**, *156*, 244.
- [17] C. P. F. O'Donnell, P. G. Davis, R. Lau, P. A. Dargaville, L. W. Doyle, C. J. Morley, *Arch. Dis. Child. Fetal Neonat. Ed.* **2005**, *90*, F392.
- [18] F. E. Wood, C. J. Morley, J. A. Dawson, C. O. F. Kamlin, L. S. Owen, S. Donath, P. G. Davis, *Arch. Dis. Child. Fetal Neonat. Ed.* **2008**, *93*, F235.
- [19] D. Cheung, Q. Mian, P. Y. Cheung, M. O'Reilly, K. Aziz, S. Van Os, G. Pichler, G. M. Schmölzer, *J. Perinatol.* **2015**, *35*, 464.
- [20] E. O'Curraïn, J. E. O'Shea, L. McGrory, L. S. Owen, O. Kamlin, J. A. Dawson, P. G. Davis, M. Thio, *Resuscitation* **2019**, *134*, 91.
- [21] J. E. O'Shea, M. Thio, L. S. Owen, C. Wong, J. A. Dawson, P. G. Davis, *Arch. Dis. Child. Fetal Neonat. Ed.* **2016**, *101*, F294.
- [22] E. Arzt, S. Gorb, R. Spolenak, *Proc. Natl. Acad. Sci. U. S. A.* **2003**, *100*, 10603.
- [23] Q. Jiang, S. Song, J. Zhou, Y. Liu, A. Chen, Y. Bai, J. Wang, Z. Jiang, Y. Zhang, H. Liu, J. Hua, J. Guo, Q. Han, Y. Tang, J. Xue, *Adv. Wound Care* **2020**, *9*, 357.
- [24] L. S. Barros, P. Talaia, M. Drummond, R. Natal-Jorge, *J. Bras. Pneumol.* **2014**, *40*, 652.
- [25] Z. Lei, J. Yang, Z. Zhuang, *J. Occup. Environ. Hyg.* **2012**, *9*, 46.
- [26] Y.-K. Lee, Z. Xi, Y.-J. Lee, Y.-H. Kim, Y. Hao, H. Choi, M.-G. Lee, Y.-C. Joo, C. Kim, J.-M. Lien, I.-S. Choi, *Sci. Adv.* **2020**, *6*, eaax6212.
- [27] L. Wang, S. Qiao, S. Kabiri Ameri, H. Jeong, N. Lu, *J. Appl. Mech.* **2017**, *84*, 111003.
- [28] Y. Wang, Y. Qiu, S. K. Ameri, H. Jang, Z. Dai, Y. Huang, N. Lu, *Npj Flex. Electron.* **2018**, *2*, 6.
- [29] Q. Wang, X. Zhao, *Sci. Rep.* **2015**, *5*, 8887.
- [30] R. Zhao, S. Lin, H. Yuk, X. Zhao, *Soft Matter* **2018**, *14*, 2515.
- [31] Y. Cho, J. H. Shin, A. Costa, T. A. Kim, V. Kunin, J. Li, S. Y. Lee, S. Yang, H. N. Han, I. S. Choi, D. J. Srolovitz, *Proc. Natl. Acad. Sci. U. S. A.* **2014**, *111*, 17390.
- [32] M. Konaković, K. Crane, B. Deng, S. Bouaziz, D. Piker, M. Pauly, *ACM Trans. Graph.* **2016**, *35*, 1.
- [33] G. P. T. Choi, L. H. Dudte, L. Mahadevan, *Nat. Mater.* **2019**, *18*, 999.
- [34] Y.-J. Lee, S.-M. Lim, S.-M. Yi, J.-H. Lee, S. Kang, G.-M. Choi, H. N. Han, J.-Y. Sun, I.-S. Choi, Y.-C. Joo, *Extreme Mech. Lett.* **2019**, *31*, 100516.
- [35] H. Yeon, H. Lee, Y. Kim, D. Lee, Y. Lee, J.-S. Lee, J. Shin, C. Choi, J.-H. Kang, J. M. Suh, H. Kim, H. S. Kum, J. Lee, D. Kim, K. Ko, B. S. Ma, P. Lin, S. Han, S. Kim, S.-H. Bae, T.-S. Kim, M.-C. Park, Y.-C. Joo, E. Kim, J. H. Han, J. Kim, *Sci. Adv.* **2021**, *7*, eabg8459.
- [36] A. K. Dabrowska, G. M. Rotaru, S. Derler, F. Spano, M. Camenzind, S. Annaheim, R. Stämpfli, M. Schmid, R. M. Rossi, *Skin Res. Technol.* **2016**, *22*, 3.
- [37] J. L. Sparks, N. A. Vavalle, K. E. Kasting, B. Long, M. L. Tanaka, P. A. Sanger, K. Schnell, T. A. Conner-Kerr, *Adv. Skin Wound Care* **2015**, *28*, 59.
- [38] C. Guerra, C. J. Schwartz, *Tribol. Lett.* **2011**, *44*, 223.
- [39] J. W. Jeong, W. H. Yeo, A. Akhtar, J. J. S. Norton, Y. J. Kwack, S. Li, S. Y. Jung, Y. Su, W. Lee, J. Xia, H. Cheng, Y. Huang, W. S. Choi, T. Bretl, J. A. Rogers, *Adv. Mater.* **2013**, *25*, 6839.
- [40] S. Wang, M. Li, J. Wu, D. H. Kim, N. Lu, Y. Su, Z. Kang, Y. Huang, J. A. Rogers, *J. Appl. Mech. Trans. ASME* **2012**, *79*, 031022.
- [41] Y. Wang, C. Gregory, M. A. Minor, *Soft Robot.* **2018**, *5*, 272.
- [42] J. Ochshorn, *J. Archit. Eng.* **2009**, *15*, 139.
- [43] Z. Lei, J. Yang, Z. Zhuang, *Comput.-Aided Des. Appl.* **2010**, *7*, 847.
- [44] F. E. Wood, C. J. Morley, J. A. Dawson, C. O. F. Kamlin, L. S. Owen, S. Donath, P. G. Davis, *Arch. Dis. Child. Fetal Neonat. Ed.* **2008**, *93*, F230.
- [45] F. E. Wood, C. J. Morley, J. A. Dawson, P. G. Davis, *Arch. Dis. Child. Fetal Neonat. Ed.* **2008**, *93*, F380.





## Supporting Information

for *Adv. Mater. Technol.*, DOI: 10.1002/admt.202101364

Reverse-Engineered Highly Conformable, Leak and Pressure Reducing Cushion for Neonatal Resuscitation Mask

*Carolyn M. McGann, Young-Joo Lee, Se-Um Kim, Danielle D. Weinberg, Xincheng Zha, Matthew Huber, Michael W. Hast, Kayley Dear, Vinay Nadkarni, Elizabeth E. Foglia,\* and Shu Yang\**

## Supporting Information

### Reverse-engineered Highly Conformable, Leak and Pressure Reducing Cushion for Neonatal Resuscitation Mask

Carolyn M. McGann, Young-Joo Lee, Se-Um Kim, Danielle D. Weinberg, Xincheng Zha, Matthew Huber, Michael W. Hast, Kayley Dear, Vinay Nadkarni, Elizabeth E. Foglia\*, Shu Yang\*

Dr. C McGann, D. Weinberg, M. Huber, Dr. E. Foglia  
Division of Neonatology, The Children's Hospital of Philadelphia, 3401 Civic Center Blvd.  
Philadelphia, PA, 19104, United States

Dr. Y-J. Lee, S-U.Kim, X. Zha, Dr. S. Yang  
Departments of Materials Science and Engineering, University of Pennsylvania, 3231 Walnut  
Street, Philadelphia, PA, 19104, United States

Dr. M. Hast, K. Dear  
Biedermann Laboratory for Orthopaedic Research, University of Pennsylvania, 3737 Market  
Street, Philadelphia, PA, 19104, United States

Dr. V. Nadkarni  
Anesthesia, Critical Care and Pediatrics, The Children's Hospital of Philadelphia, 3401 Civic  
Center Blvd., Philadelphia, PA, 19104, United States

E-mails: [shuyang@seas.upenn.edu](mailto:shuyang@seas.upenn.edu) and [FOGLIA@chop.edu](mailto:FOGLIA@chop.edu)

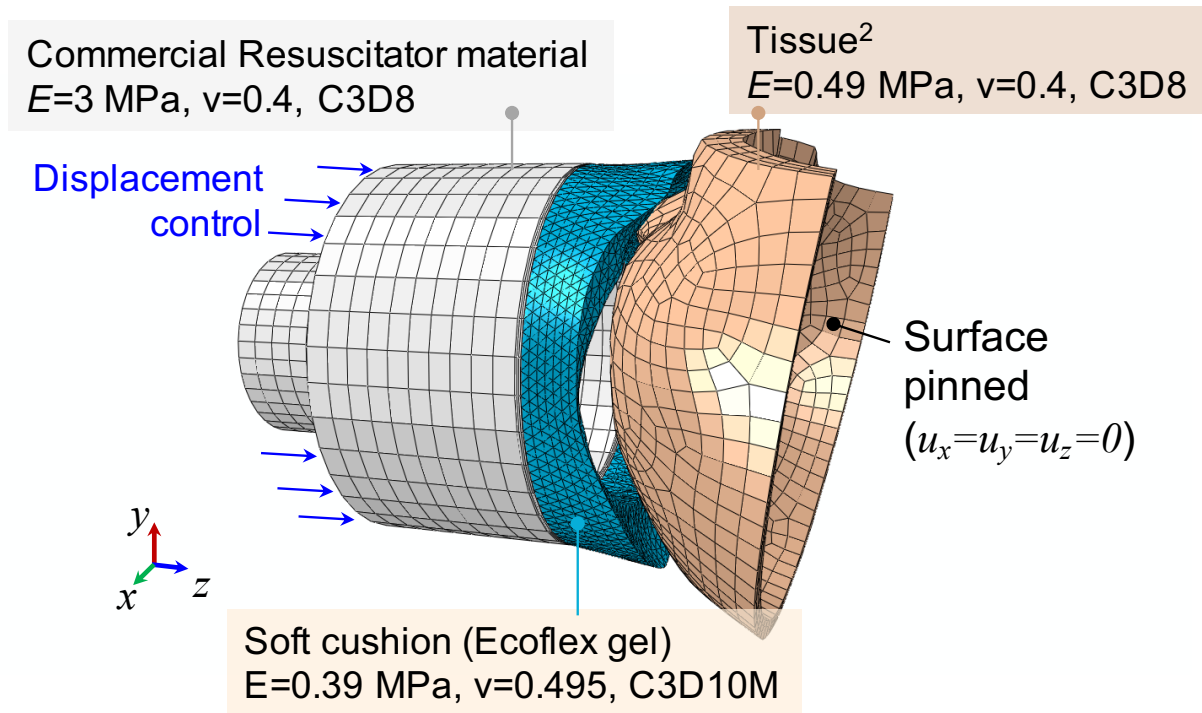


**Figure S1.** Schematic illustration of the boundary conditions of finite element simulation for mask integration.

**Reference:**

1. Y. Wang, C. Gregory, M. A. Minor, Improving mechanical properties of molded silicone rubber for soft robotics through fabric compositing. *Soft Robot.* **5**, 272–290 (2018).
2. Z. Lei, J. Yang, Z. Zhuang, Headform and N95 filtering facepiece respirator interaction: Contact pressure simulation and validation. *J. Occup. Environ. Hyg.* **9**, 46–58 (2012).